Telecommunications and Radio Engineering, 67(19):1749-1762 (2008)

SOLID-STATE ELECTRONICS

Quantum Efficiency of the InGaAS/GaAs Resonant Photodetector for the Ultrashort Optical Connections*

S.V. Gryshchenko, A.A. Dyomin, V.V. Lysak, and S.I. Petrov

Kharkiv National University of Radio Engineering and Electronics,
14, Lenin Ave, Kharkiv, 61166, Ukraine

ABSTRACT: A theoretical analysis has been conducted for the quantum efficiency of an InGaAs/GaAs resonant cavity *p-i-n* photodetector for the ultrashort optical connections. The quantum efficiency at resonance has been estimated. The mathematical model allows for the physical parameters of the photodetector, radiation wavelength, mirror reflectivity and optical absorption in all detector layers. The relations between the quantum efficiency and the reflection coefficient of the upper mirror of the $Al_{0.65}Ga_{0.35}As$/GaAs resonator in combination with other variable parameters of the structure have been determined. The magnitudes of the upper mirror reflection coefficient depending on physical parameters of the structure have been found.

The rapid growth of computer technologies makes new demands to the high-speed communication systems, including the ultrashort connections. The state-of-the-art computers utilize optical connections not only instead of stubs but also instead of electron logical elements of the motherboard. Thus, the research on the optical connection elements (receiver, transmitter, waveguide) is still on the agenda. Among the transmitters, the vertical resonator lasers (VRL) are the most attractive choice. The receivers of the laser radiation are *p-i-n* photodiodes, distinguished by a high response speed and the frequency characteristic being shifted to the higher frequency range in relation to other types of photodiodes [1-4]. Good promises show also the resonant cavity photodetectors (RCPD), whose *p-i-n* structure is embedded into an optical resonator with the mirrors, as a

* Originally published in *Radiophysics and Electronics*, Vol. 12, No 2, 2007, pp. 401–407.

ISSN 0040-2508

rule, being the Bragg reflectors. The advantage of this engineering solution is that the optical field is amplified at the resonance frequency inside RCPD. By a small *i*-region, the achievable quantum efficiency is very high. For example, at the order of dozens of nanometer it is almost 100% [1,2,5,6]. Hence, the response speed of the diode that depends on the *i*-region width remains high. Having a high response speed and perceptibility toward the required narrow oscillation spectrum, RCPDs are the most suitable devices for data transmission systems. The QE parameter (η) actually indicates the efficiency of transformation of the optical power into the electric one and is the key factor for all types of photodetectors. The QE magnitude depends on the physical parameters of the detector and the resonator mirrors. The investigation of these dependences determines the aim and the problems stated in this work.

The aim of presented paper is to explore the influence of the physical parameters of a resonance cavity detector on its quantum efficiency. The necessary values of the reflection coefficient to provide the high QE should be achieved allowing for the given detector material and the wavelength to be detected.

The problem to be solved is building, by means of the analytical model, the dependence of QE on the reflection coefficient of the resonator mirrors, the efficient layer width and the absorption coefficients. The results should be analyzed to reveal the mechanism of controlling the QE by varying the physical parameters. The obtained dependences will be used to determine the necessary number of layers in the upper Bragg reflector that will ensure a high QE.

MATHEMATICAL MODEL

The quantum efficiency of the detector is defined as a probability for a photon inside the detector to excite an electron that would produce the photocurrent. The total QE includes the optical QE, taking into account the photon absorption in the substance, the internal QE, taking into account the inelastic electron scattering in the quantum well, and the barrier QE, taking into account the electron scattering at the contact barrier.

In view of the above, we can write down the total QE

$$\eta = \eta_a \eta_b \eta_c , \tag{1}$$

where η_a is the optical QE, η_b is the barrier QE, η_c is the internal QE.

The diagram of RCPD is presented in Fig. 1. The efficient absorbing layer is situated between two distributed Bragg reflectors (DBR) and is determined by the thickness d and the absorption coefficient α. The distances between the efficient layer and the upper and the bottom mirrors are denoted with L_1 and L_2,

respectively, that means the length of the separating layer. The case in question concerns a direct incidence of the radiation on the photodetector, so we confine the consideration to the one-dimensional variant. Assume that the tangential component of the electric vector incident on the photodetector is E_i. By using the plane wave approximation, decompose the electromagnetic field in the RCPD structure into the forward wave E_f and the back wave E_b. The resonator mirrors, the upper and the bottom ones, are described by the amplitude reflection coefficients $r_1 e^{-j\varphi_1}$ and $r_2 e^{-j\varphi_2}$, respectively, where φ_1 and φ_2 are the phase shifts conditioned by the optical field penetration inside the mirror; r_1 and r_2 are the absolute values of the amplitude reflection coefficients. The energy reflection coefficients of the upper and the bottom mirrors are expressed as $R_1 = r_1^2$ and $R_2 = r_2^2$, respectively.

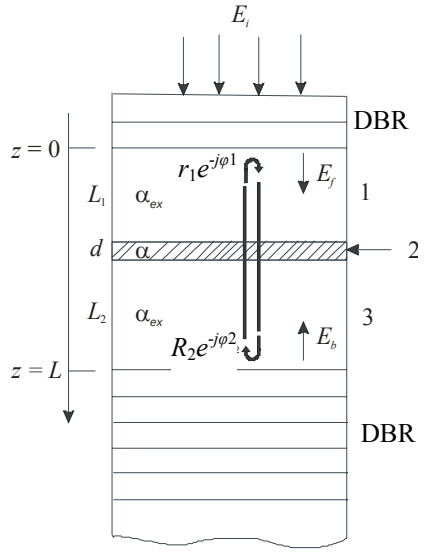

FIGURE 1. Shematic view of the resonance cavity detector: 1 and 3 are the separating layers, 2 is the efficient layer.

The forward wave E_f at the point $z = 0$ can be obtained from the self-consistence condition, i.e., E_f is the total of the wave transmitted through the upper mirror and the wave transmitted through the whole resonator forth and back. Thus, the expression for E_f can be presented as a self-consistent equation [1,5,6]

$$E_f = t_1 E_i + r_1 r_2 e^{-\alpha d - \alpha_{ex}(L_1+L_2)} \times e^{-j(2\beta L + \varphi_1 + \varphi_2)} E_f, \qquad (2)$$

where t_1 is the transmission factor of the upper DBR; α is the absorption coefficient of the efficient layer; α_{ex} is the absorption coefficient of the separating layer; β is the propagation constant.

According to (2), the forward wave E_f is written as

$$E_f = \frac{t_1}{1 - r_1 r_2 e^{-\alpha d - \alpha_{ex}(L_1+L_2)} e^{-j(2\beta L + \varphi_1 + \varphi_2)}} E_i .$$

The back wave E_b has the form

$$E_b = r_2 e^{-\alpha d/2} e^{-(\alpha_{ex}/2)(L_1+L_2)} e^{-j(\beta L + \varphi_2)} E_f . \tag{3}$$

The optical power inside the resonator is [1]

$$P_s = \frac{n}{2\eta_0} |E_s|^2 , \text{ (where } s = f \text{ or } b\text{)}, \tag{4}$$

where η_0 is the vacuum impedance; n is the refraction index of the detector material.

Here, the optical power absorbed in the efficient layer P_l can be derived from the input power P_i in the following form [1,7,8]:

$$\begin{aligned} P_l &= \left(P_f e^{-\alpha_{ex} L_1} + P_b e^{-\alpha_{ex} L_2}\right)\left(1 - e^{-\alpha d}\right) = \\ &= \frac{\left(1 - r_1^2\right)\left(e^{-\alpha_{ex} L_1} + r_2^2 e^{-\alpha_{ex} L_2} e^{-\alpha_c L}\right)\left(1 - e^{-\alpha d}\right)}{1 - 2 r_1 r_2 e^{-\alpha_c L} \cos\left(2\beta L + \varphi_1 + \varphi_2\right) + \left(r_1 r_2\right)^2 e^{-2\alpha_c L}} P_i , \end{aligned} \tag{5}$$

where α_C is the normalized absorption coefficient equal to $\alpha_c = \left(\alpha_{ex} L_1 + \alpha_{ex} L_2 + \alpha d\right)/L$.

Bearing in mind that the optical QE is

$$\eta_a = P_l \Big/ P_i , \tag{6}$$

obtain

$$\eta_a = \left(1 - R_1\right)\left(1 - e^{-\alpha d}\right) \frac{\left(e^{-\alpha_{ex} L_1} + e^{-\alpha_{ex} L_2} R_2 e^{\alpha_c L}\right)}{\left[1 - 2\sqrt{R_1 R_2} e^{-\alpha_c L} \cos\left(2\beta L + \varphi_1 + \varphi_2\right) + R_1 R_2 e^{-2\alpha_c L}\right]} . \tag{7}$$

As can be easily seen from (7), QE has a periodical spectrum. The peak QE will be observed at the resonance wavelength. At the resonance, $\left(2\beta L+\varphi_1+\varphi_2=2m\pi\ (m=1,2,3...)\right)$, expression (7) can be reduced to

$$\eta_a=\left(\frac{\left(e^{-\alpha_{ex}L_1}+e^{-\alpha_{ex}L_2}R_2e^{\alpha_c L}\right)}{\left[1-\sqrt{R_1R_2}e^{-\alpha_c L}\right]^2}\right)\times\left(1-R_1\right)\left(1-e^{-\alpha d}\right). \tag{8}$$

It should be noted that in eq. (8) the reflections at the boundary surfaces between the efficient layer and the separating layers are neglected. This approximation is true when the considered object is a heterostructure with small contrasts of the dielectric constant [1,3,7].

The influence of the standing wave (SW), i.e., the spatial distribution of the optical field in the resonator, is also neglected in this equation. While dealing with detectors having thick efficient layers covering several SW periods, one can neglect the SW influence. However, the SW contribution is considerable for very thin efficient layers [8].

The SW contribution can be taken into account by using the concept of an efficient absorption coefficient [1,8]

$$\alpha_{eff}=SWC\cdot\alpha, \tag{9}$$

where SWC is the corrected SW coefficient; α_{eff} is the efficient absorption coefficient in the efficient region, taking into account the SW influence. Substituting α by α_{eff} in (8), we obtain QE that allows for SW.

For a case when $\varphi_1=0$, $\varphi_2=0$, i.e., the radiation wavelength corresponds to the Bragg mirror wavelength $\lambda=\lambda_B$, and $L_1=L_2$, i.e., the efficient layer is situated directly in the center of the resonator, one can apply the following formula for SWC [8]:

$$SWC=1+\frac{2\mathrm{r}_2\sin\left(\beta d\right)}{\beta d\left(1+r_2^2\right)}, \tag{10}$$

where $\beta=\frac{2\pi n_{eff}}{\lambda}$; $n_{eff}=\frac{L_1n_1+L_2n_2+dn_a}{L}$ is the efficient refraction index, n_1, n_2 and n_a are the refraction indices of the separating and the efficient layer.

The internal QE parameter should be considered only when the photodetector contains quantum-dimensional layers. The optically excited electrons in the efficient layer will experience an inelastic scattering, as a result

lose their energy, thus the probability of escaping the potential well will decrease. The parameter can be presented in the form

$$\eta_c = \exp(-d / L_z), \tag{11}$$

where L_z is the free path length of the electron.

The barrier QE is defined as a probability for the electron to run a distance of x near the barrier without scattering

$$\eta_b = \exp(-x / L_s), \tag{12}$$

where L_s is the free path length in the potential well created by force of "electric image"; x is the distance between the barrier peak and the boundary. The force of "electric image" characterizes the interaction between the electric charges and the boundary of two semiconductors [9].

The location and the height of the barrier peak depends on the applied bias voltage, as the external field changes the force of "electric image" [10]. As a result, the dependence of the photocurrent on the bias voltage is conditioned by the electron scattering in the potential well at the boundary and by the variation of the maximum barrier energy. Distance x can be presented as [10]

$$x = \left(\frac{q}{16\pi\varepsilon_0\varepsilon_a F} \right)^{1/2}, \tag{13}$$

where q is the electron charge, ε_0 is the dielectric constant, ε_a is the dielectric permittivity of the efficient layer, $F = (V_b - V_0)/d$ is the electric field in the efficient region, V_b is the bias voltage, V_0 is the plane region energy.

THE STRUCTURE UNDER INVESTIGATION

The detecting structure is a three-layered $In_{0.2}Ga_{0.8}As/GaAs$ compound, whose optical length is a half-wavelength of the incident radiation ($\lambda = 0.98$ μm). The structure and the materials were chosen on the basis of experimental data obtained by various research teams, with the regard of the information on actual devices [3-5,11-13]. The diagrammatic view of the structure in question is shown in Fig. 2.

The choice of $In_{0.2}Ga_{0.8}As$ as the active material was conditioned by the presence of the absorption peak in the region of 1 μm, since much of the radiators used in the data transmission systems, operate in this very spectral range. The separating layer material was chosen to be GaAs, in the first place,

due to the minor absorption at the operating wavelength [2,3]. For DBR we selected a multilayered mirror $Al_{0.65}Ga_{0.35}As/GaAs$. This structure is characterized by low barrier voltages, high heat conductance, high electric conductance, the required contrast of the refraction indices, low losses of the radiation absorption at the free carriers and the possibility to apply the methods of the current and optical field transverse limiting. The thickness of the Bragg mirror layers was selected such that the Bragg mirror wavelength λ_B was $0.98\,\mu m$.

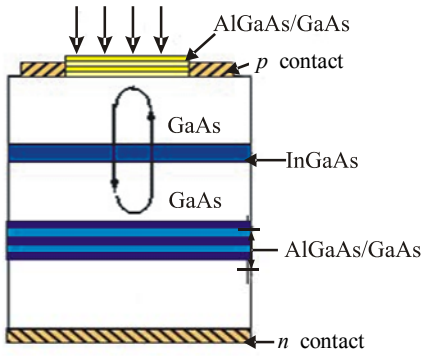

FIGURE 2. The structure under investigation.

The Table 1 lists the parameters used for the numerical modeling of QE and the reflectance of DBR.

Table 1: Structure parameters

Parameter	Value
Efficient layer thickness, d ($In_{0.2}Ga_{0.8}As$)	from 4 to 15 nm
Separating layer thickness, h (GaAs)	from 61 to 67 nm (depending on d value)
Mirror layer thickness ($Al_{0.65}Ga_{0.35}As$)	77.44 nm
Mirror layer thickness (GaAs)	69.5 nm
Refraction index $Al_{0.65}Ga_{0.35}As$	3.1637
Refraction index GaAs, n_1, n_2	3.5256
Refraction index $In_{0.2}Ga_{0.8}As$, n_a	3.5691
Absorption coefficient of the efficient region, α ($In_{0.2}Ga_{0.8}As$)	from $1.5\cdot10^4$ to $24\cdot10^4$ cm^{-1}
The absorption coefficient of the separation layer, α_{ex} (GaAs)	$1.5\cdot10^2$ cm^{-1}
Plane wave energy, V_0	2.1 V
Carrier free path length, L_z	250 A

RESULT ANALYSIS

Figures 3 and 4 demonstrate the computation results for QE as a function of the upper mirror reflection coefficient R_1 for various values of the bottom mirror reflection coefficient R_2. The graphs are built for two values of the efficient layer absorption coefficient at the resonance. According to the computations, the only dependence having a peak is QE v.v. R_1, hence below we will consider this dependence for various values of other structure parameters. The value of R_1 at the peak of QE depends on R_2. To reach the maximum QE, R_1 should be decreased simultaneously with R_2. The maximum amplification in the resonator could be reached provided that the radiation is retained in the central part, i.e., the condition $R_2 > R_1$ should be satisfied.

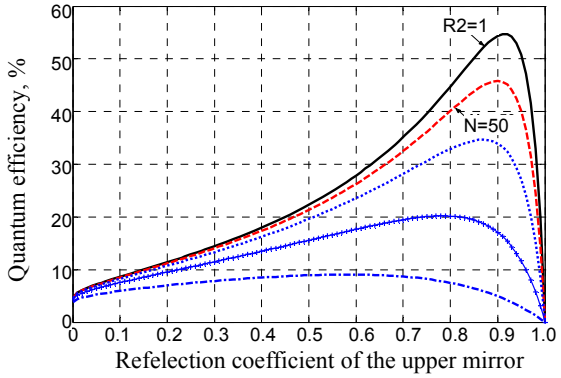

FIGURE 3. Dependence of QE on the reflection coefficient of the upper and the bottom mirrors for $\alpha = 1.5 \cdot 10^4$ cm^{-1}. The number in brackets denotes the DBR layers for the bottom mirror. The solid curve corresponds to $R_2 = 1$ at $N = \infty$. The rest of curves top-down $R_2 = 0.98(N = 50)$; $R_2 = 0.95(N = 40)$; $R_2 = 0.86(N = 30)$; $R_2 = 0.63(N = 20)$.

As seen from the graphs, η decreases as R_2 goes down at any value of R_1. The reason is that while decreasing R_2, the losses increase considerably, as a part of radiation after every passage inside the resonator leaves it through the bottom mirror. Due to the quantum-dimensional nature of the efficient layer, the absorption per one passage is very small. Hence, the reflection coefficient of the bottom mirror should be as high as possible. Interesting moment is that the stronger the influence of the R_2 magnitude on QE, the lower the absorption coefficient in the efficient layer (compare the curve bias in Figs. 3 and 4), as

during one passage the ratio between the absorption in the efficient layer and the losses at the bottom mirror will become smaller.

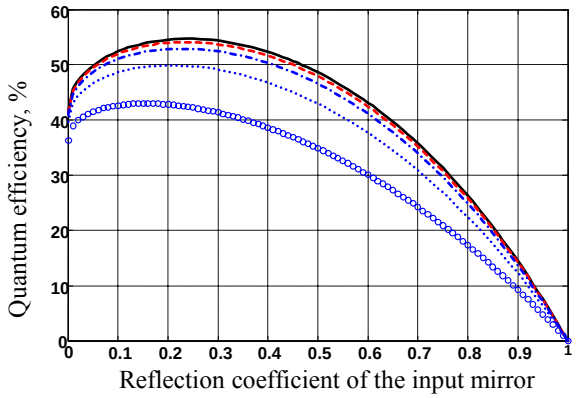

FIGURE 4. Dependence of QE on the reflection coefficient of the upper and the bottom mirrors for $\alpha = 24 \cdot 10^4$ cm^{-1}. The number in brackets denotes the DBR layers for the bottom mirror. The solid curve corresponds to $R_2=1$ at $N=\infty$. The rest of curves top-down $R_2=0.98(N=50)$; $R_2=0.95(N=40)$; $R_2=0.86(N=30)$; $R_2=0.63(N=20)$.

As known, the reflection coefficient grows as the number of the DBR layers increases [2,12], that is shown in Fig. 5, illustrating the dependence between the reflection coefficient of the bottom mirror and the layer number. Obviously, by a small number of layers, the dependence is almost linearly ascending. It enables one to obtain a relatively high reflection coefficient by simple adding layers to the bottom DBR. However, when the layers are more than 15, an inflection of the curve occurs and the growth of the reflection coefficient slows down. The reflection of every individual layer diminishes due to their bigger total number, which causes the saturation. Thus, the 100% reflection can hardly be achieved just by adding new layers. The unlimited piling of the DBR layers will lead to the increase in the production cost and growth of the optical losses in DBR. So the reflection coefficient of $R_2 = 0.98$ for the exit mirror seems to be sufficient [3,4,13]. This value can be reached by the layer number $N = 50$. Even more efficient method of obtaining the maximum-close-to-unity reflection coefficient implies usage of materials with a high refraction index contrast [14].

The reflection coefficient in the multiple DBR layers, i.e., the external layers, the substrate and the separating layers, were taken into account as well. As distinct from the bottom mirror, air is also numbered among the external layers of the upper one, so that the contrast of the air-AlGaAs refraction index is quite high. It causes an essential increase in the mirror reflection coefficient by the same number of layers (Fig. 6), enabling one to reduce their number.

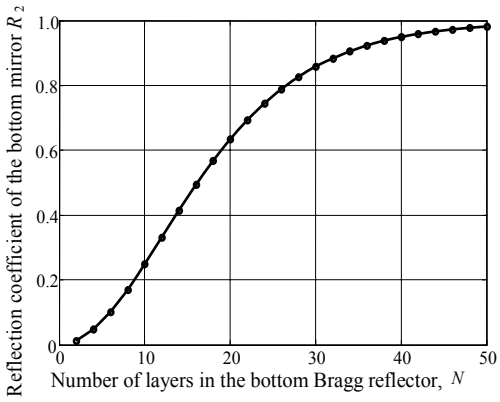

FIGURE 5. Dependence of the reflection coefficient of the bottom mirror on the DBR layer number.

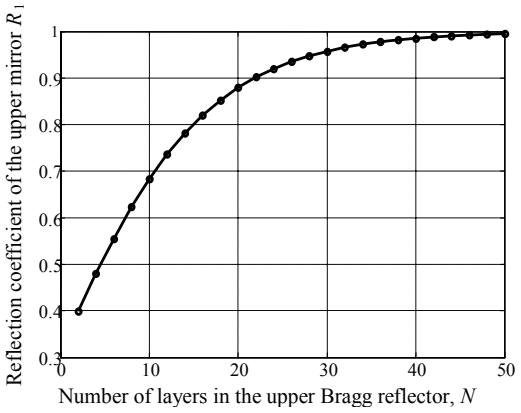

FIGURE 6. Dependence of the reflection coefficient of the upper mirror on the DBR layer number.

Now let us consider how the thickness of the efficient layer influences the QE. Figure 7 shows that QE increases with the efficient layer getting thinner. This result is true solely for detectors with quantum-dimensional efficient layers, because the total QE includes the optical and the internal quantum efficiencies. According to the theory, for the massive-semiconductor-based detectors, the thicker the efficient layer, the higher the optical QE [2]. For the detectors having quantum-dimensional efficient layers, the contribution of the internal QE is

relevant (11), which increases in inverse proportion to the efficient layer thickness and has a more pronounced effect on the total QE by minor variations of the efficient layer thickness. The QE peak shifts toward higher reflection coefficient R_1. This can be explained by a reduced absorption in the efficient region during a single radiation passage through the efficient layer, and consequently the possibility to perform more passages due to the enhanced reflectivity of the upper mirror.

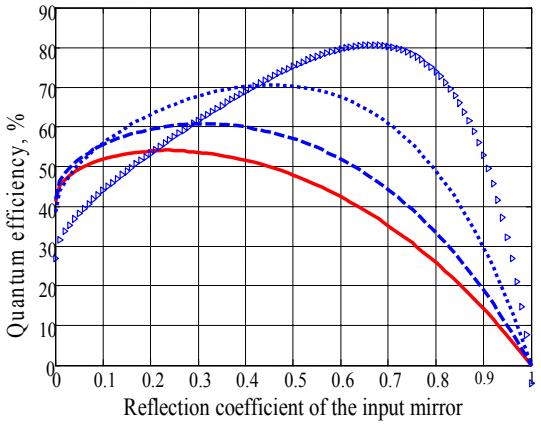

FIGURE 7. Dependence between QE and the reflection coefficient of the upper mirror by various thickness of the efficient layer. The solid curve corresponds to $d = 15$ nm, the dashed one to $d = 12$nm, the dotted one to $d = 8$ nm, the cross-marks to $d = 4$ nm.

Figure 8 presents the relation between QE and the reflection factor of the upper mirror for various optical absorption coefficients of the efficient layer. The QE grows predictably by a stronger absorption. At the same time, the QE peak moves toward lower reflection coefficients of the upper mirror. The reasons to such behavior are as follows. One of the conditions of a low back reflection of the detector radiation at the resonance wavelength is the multibeam interference within the resonator. The multiple radiation passing from mirror to mirror is very important here. By a strong increase of the absorption in the efficient region, the number of passages drops and no sufficient interference can be achieved. Consequently, the reflection from the detector is high and, correspondingly, the Q-factor is low. The less the reflection from the upper mirror, the less the necessary number of passages, and as a result the Q-factor and QE increase. If the optical absorption is low, more radiation passages are required for a complete absorption in the efficient layer. Thus, the reflection coefficients should be high to provide a high Q-factor.

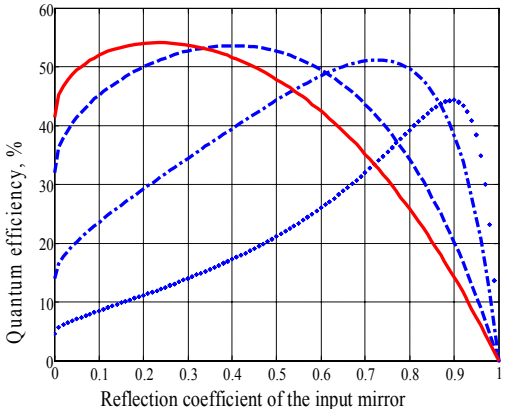

FIGURE 8. Dependence between QE and the reflection coefficient of the upper mirror by various absorption coefficients of the efficient layer. The solid curve corresponds to $\alpha = 1.5$ μm^{-1}, the dotted one to $\alpha = 5$ μm^{-1}, the dashed one to $\alpha = 15$ μm^{-1}, the circle-marks to $\alpha = 24$ μm^{-1}.

The calculations have proven that the influence of the absorption coefficients of the separating layers on QE of RCPD is negligible. It was also revealed that the barrier quantum efficiency can amount to almost 100% provided that the bias voltage is chosen properly [15].

CONCLUSION

The task of analyzing the dependence between the physical parameters of the resonant cavity detector and its quantum efficiency has been successfully completed. The calculations have revealed that:

- the dependence of QE versus the reflection factor of the upper mirror has an extreme function. By quite a high absorption, the peak of the characteristic corresponds to a low reflection coefficient of the upper mirror (QE = 54.1% for $\alpha = 24 \cdot 10^4$ cm^{-1}, $d = 15$ nm, $R_2 = 0.98$ and $R_1 = 0.24$) (the role of the upper mirror can be played by the reflection from the air-semiconductor boundary [1]);
- the further growth of the total QE is hindered by the low internal QE due to the quantum effects in the efficient layer. A high QE can be achieved by reducing the efficient layer thickness (QE = 80.7% for $\alpha = 24 \cdot 10^4$ cm^{-1}, $d = 4$ nm, $R_2 = 0.98$ and $R_1 = 0.67$, i.e., ten layers of the upper mirror suffice);

- the bottom mirror should have the maximum possible reflection coefficient. By a reduced number of the layers in the bottom mirror, the number of the upper mirror layers should be reduced correspondingly in order to maintain the required QE;
- QE drops when the absorption in the efficient layer weakens, but a relative decrease can be registered only when the absorption coefficient reduces by an order. In this case the requirements to the reflectivity of the upper mirror are drastically changed (QE = 54.1% for $\alpha = 24 \cdot 10^4$ cm^{-1} and $R_1 = 0.24$ against QE = 44.3% for $\alpha = 1.5 \cdot 10^4$ cm^{-1} and $R_1 = 0.9$).

This research has yielded the numerical results on the reflection coefficient of the upper mirror for the given materials the detector is made off and the detected radiation wavelength, which are new for this area of investigation. The understanding of the relation between the physical parameters of the structure and QE is highly important for creating new RCPD designs and improving the existing ones.

We have analyzed the influence of the physical parameters of the structure on the quantum efficiency at the resonance only. However, a more detailed specification should also allow for the non-resonant case where the wavelength dependence is relevant. The above considered analytical model is inapplicable for more in-depth studies, so one should resort to the methods of QE estimation based on the intrinsic electromagnetic field calculation.

ACKNOWLEDGEMENT

The authors would like to express their sincere acknowledgement to I.A. Sukhoivanov for his valuable advice concerning the research and assistance in elaboration of the manuscript.

REFERENCES

1. Selim Unlu, M., and Strite, S., (1995), Resonant Cavity enhanced photonic devices, *J. Appl. Phys*. **78**(2):230-234.
2. Kies, R.J., Kruse, P.W., Patly, P.W., et al., (1985), *Photoreceivers of visible and IR range*, Radio i Svyaz, Moscow: 328 p.
3. Xie, K., Zhao, J.H., Shi, Y., at al., (1996), Resonant Cavity Enhanced GaInAsSb-AlAsSb Photodetector Grown by MBE for Mid-IR Applications, *IEEE Photonics Technology Letters*. **8**(5):1230-1234.
4. Tailor, G.W, Simmons, J.G., Cho, A.Y., and Mand, R.S., (1986), A new double-heterostructure optoelectronic switching device using molecular-beam epitaxy, *J. Appl. Phys*. 59:230-234.

5. Gryshchenko, S.V., and Klimenko, M.V., (2006), Analysis of the quantum efficiency of a resonant GaAs photodetector, *10 Yubil. Mezhdun. Molodezhn. Forum "Radioelektronika i Molodezh v XXI st."*, KhNURE, Kharkov: 161 p. (in Russian).
6. Kafai, Lai, and Campbell Joe, C., (1994), Design of a Tunable GaAs/AlGaAs Multiple-Quantum-Well Resonant-Cavity Photodetector, *IEEE J. of Quantum Electronics*. **30**(1):108-114.
7. Soboleva, N.A., and Melamid, A.Y., (1974), *Photoelectronic devices*, Vyshsaya Shkola, Moscow: 376 p. (in Russian).
8. Zhang, Y.H., Luo, H.T., and Shen, W.Z., (2002), Study on the quantum efficiency of resonant cavity enhanced GaAs far-infrared detectors, *J. Appl. Phys*. **91**(9):5538-5544.
9. Strikha, V.I., (1982), *Contact phenomena in semiconductors*, Vyshsaya Shkola, Kiev:224 p. (in Russian).
10. Perera, A.G.U., Yuan, H.X., and Francombe, M.H., (1995), Homojunction internal photoemission far-infrared detectors: Photoresponse performance analysis, *J. Appl. Phys*. **77**(2):915-924.
11. Jervase Joseph, A., and Bourdoucen, Hadj, (2000), Design of Resonant-Cavity-Enhanced Photodetectors Using Genetic Algorithms, *IEEE J. of Quantum Electronics*. **36**(3):325-332.
12. Knodl, T., Choy, H.K., Pan, J.L. at al., (1999), RCE Photodetectors Based on VCSEL Structures, *IEEE Photonics Technology Letters*. **11**(10):1289-1291.
13. De Corby, R.G., Hnatiw, A.J.P., and Hillier, G., (1999), Resonant-Cavity MSM Photodetector Employing a Burstein-Shifted InGaP-GaAs Reflector, *IEEE Photonics Technology Letters*. **11**(9):1165-1167.
14. Kovbasa, A.A., Zin'kovskaya, I.O., Lysak, V.V., et al., (2005), Reflecting properties of the distributed Bragg reflectors conjoint with an oxide window, *Radioelektronika and Informatika*. 3:55-61 (in Russian).
15. Gryshchenko, S.V., and Dyomin, A.A., (2007), Influence of image forces on the motion of electrons in the heterostructure InGaAs/GaAs, *11 Yubil. Mezhdun. Molodezhn. Forum "Radioelektronika i Molodezh v XXI st."*, KhNURE, Kharkov:293 p. (in Russian).